JCTC Journal of Chemical Theory and Computation

Theoretical Mechanistic Study of the Oxidative Degradation of Benzene in the Troposphere: Reaction of Benzene−HO Radical Adduct with O_2

Santiago Olivella,*[,†] Albert Solé,[‡] and Josep M. Bofill[§]

Institut de Química Avançada de Catalunya, CSIC, Jordi Girona 18-26, 08034-Barcelona, Catalonia, Spain, and Departament de Química Física, Departament de Química Orgànica, and Institut de Química Teòrica i Computacional, Universitat de Barcelona, Martí i Franquès 1, 08028-Barcelona, Catalonia, Spain

Received February 16, 2009

Abstract: Competing pathways arising from the reaction of hydroxycyclohexadienyl radical (**1**) with O_2, a key reaction in the oxidative degradation of benzene under tropospheric conditions, have been investigated by means of density functional theory (UB3LYP) and quantum-mechanical (UCCSD(T) and RCCSD(T)) electronic structure calculations. The energetic, structural, and vibrational results furnished by these calculations were subsequently used to perform conventional transition-state computations to predict the rate coefficients and evaluate the product yields. The trans stereoisomer of the peroxyl radical (**4**) produced by the O_2 addition to position 2 of benzene ring in radical **1** is energetically more stable than the cis one, although the rate coefficients at 298 K for the formation of both isomers are predicted to be similar. The cyclization of the cis isomer of **4** to a bicyclic allyl radical (**5**) involves calculated barrier heights ($\Delta U^{\ddagger}$, $\Delta E^{\ddagger}$, $\Delta H^{\ddagger}$, and $\Delta G^{\ddagger}$) significantly lower than those of the cyclization of the trans isomer of **4**. This implies that the formation of the cis isomer of **4** can lead to irreversible loss of radical **1** and that the observed chemical equilibrium **1** + $O_2 \leftrightarrow$ **4** essentially involves the trans isomer of **4**. Although the reaction enthalpies computed for the O_2 addition to position 4 of benzene ring in radical **1**, affording the cis and trans stereoisomers of a peroxyl radical (**6**), are similar to those for the addition to position 2, the latter addition mode is clearly preferred because it involves lower barrier heights. The barrier heights computed for the cyclization of either the cis or the trans isomers of **6** to a bicyclic radical bearing a peroxy bridge (**7**) are about twice those computed for the cyclization of either the cis or the trans isomers of **4**. Thus, under tropospheric conditions, it is unlikely that the O_2 addition to position 4 of the benzene ring in radical **1** can contribute to the formation of benzene oxidation products.

1. Introduction

Benzene is the simplest aromatic hydrocarbon that contributes significantly to the pollution of the troposphere, especially in urban areas of industrialized countries.[1] It is mainly released into the troposphere as a result of anthropogenic activities, such as emissions from burning oil and coal, motor vehicle exhaust, and evaporation of solvents and from gasoline.[2,3] It is now recognized that benzene oxidation reactions may be responsible for a significant fraction of photochemically produced tropospheric ozone.[4] Also, the likely formation of secondary organic aerosols from the oxidation of aromatic hydrocarbons is of considerable concern in connection with human health and the climate.[5]

* Corresponding author e-mail: sonqtc@cid.csic.es.

† Institut de Quimica Avançada de Catalunya.

‡ Departament de Química Física i Institut de Química Teòrica i Computacional.

§ Departament de Química Orgànica i Institut de Química Teòrica i Computacional.

10.1021/ct900082g CCC: \$40.75
Published on Web 05/21/2009

Scheme 1

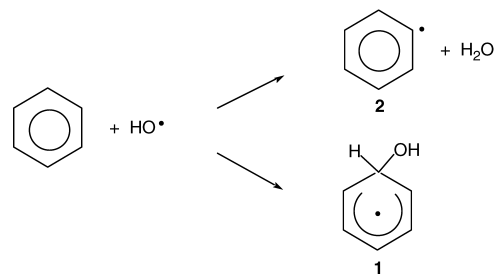

Scheme 2

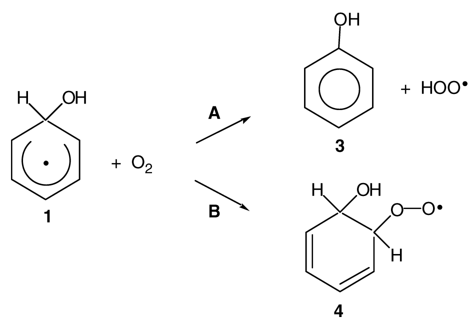

Scheme 3

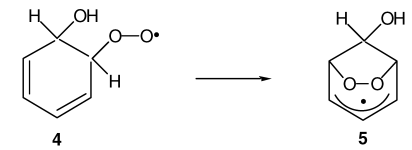

Scheme 4

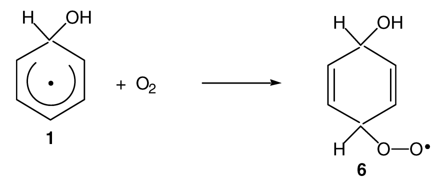

Despite its importance, the knowledge about the tropospheric degradation mechanism of benzene is still scant. Generally, the degradation of benzene in the troposphere is primarily initiated by the addition of hydroxyl radical ($HO^•$) to the aromatic ring, yielding a benzene−$HO^•$ adduct: the hydroxycyclohexadienyl radical (**1** in Scheme 1).[6−13] The H-atom abstraction from the aromatic ring leading to formation of phenyl radical (**2** in Scheme 1) is a minor process under tropospheric conditions.[13−15]

Although the benzene−HO radical adduct **1** initially formed has been found to react more rapidly with NO_2 than with NO, and even more slowly with O_2,[12,16] on the basis of the relative abundance,[17] the latter reaction is the major transformation of this radical in the troposphere.[6−8,18] The presently accepted first elementary steps of this reaction are given in Scheme 2. The reaction can proceed either by abstraction of the H-atom *gem* to HO in **1**, forming phenol (**3**) and $HOO^•$ (pathway A), or by O_2 addition to the benzene ring in **1** producing hydroxyl-2,4-cyclohexadienyl-6-peroxyl radical **4** (pathway B). Because of the relatively weak chemical bonding between the C_6H_6OH and OO fragments in peroxyl radical **4**,[6] pathway B is reversible under tropospheric conditions and leads to chemical equilibrium between **1** + O_2 and **4**.[18−22]

The peroxyl radical **4** can undergo various reaction pathways, in addition to the decomposition back to the **1** + O_2 reactants. On the basis of previous theoretical calculations,[23] the ring closure in **4** affording a bicyclic radical (**5** in Scheme 3) appears to be the only plausible unimolecular reaction for peroxyl radical **4**. It is worth noting that the bicyclic radical **5** bears a peroxy bridge and its structure is defined by two fused five- and seven-membered rings, the latter containing a delocalized allyl radical. The subsequent reaction of the bicyclic radical **5** is thought to lead to aromatic ring cleavage forming the principal benzene oxidation products (i.e., glyoxal and butenedial).[24,25]

A number of theoretical investigations have focused on characterizing the **1** + O_2 potential energy surface (PES) to explain the experimentally observed branching ratios, thermochemical properties, and rate coefficients.[6,20,22,23,26,27] One of the most thorough theoretical investigations on the primary steps of the benzene oxidation has been published by Lesclaux and co-workers.[22] By using a combination of density functional theory (DFT) and ab initio quantum mechanical calculations with a quadratic correlation (of the Marcus type[28]) between the activation barriers and the reaction enthalpies,[29] Lesclaux and co-workers predicted for the phenol channel (pathway A in Scheme 2) a formation yield of ∼55% in reasonable agreement with the experimental values (25−61%).[1,30−32] Additionally, these authors found that the chemical equilibrium between **1** + O_2 and **4** must essentially involve the trans stereoisomer of **4** (designated by **4**-*trans*), which is less energetic and is formed more rapidly (a factor of about 50) than the cis one (designated by **4**-*cis*). In contrast, the cyclization of **4**-*trans* was calculated to be too slow, as compared to the global rate of irreversible loss of **1** and **4**, whereas it is very fast in the case of **4**-*cis* and can lead readily to benzene oxidation products. However, it must be pointed out that the calculated rate coefficient for the **4**-*cis* formation is a factor of about 10 too low for being consistent with a reasonable yield of oxidation products formed through this reaction channel.[22] Therefore, the possibility of finding another (faster) reaction pathway for the formation of **4**-*cis* deserves a further investigation. Moreover, all previous theoretical studies on the reaction of O_2 with radical **1** leading to peroxyl radicals have focused on the O_2 addition to position 2 of the benzene ring in **1**.[6,20,22,23,26,27] The O_2 addition to position 4 of the benzene ring in **1** affording the hydroxyl-2,5-cyclohexadienyl-4-peroxyl radical (**6** in Scheme 4) appears to be an alternative route[33] that merits a study to elucidate whether or not it plays any relevant role in the tropospheric degradation mechanism of benzene.

New theoretical calculations, using DFT and high level ab initio methods, have been performed in this work aiming to clarify the relative rate coefficients for the formation of the cis and trans isomers of radical **4**, assess the feasibility of the reaction channel leading to the cis and trans isomers of radical **6**, and provide new data on the thermochemistry and kinetics of the reactions of radicals **1**, **4**, and **6**.

2. Computational Details

2.1. Electronic Structure Calculations. The geometries of the relevant stationary points (minima and first-order saddle points) on the lowest energy PES of the radical **1** + O_2 reaction system were optimized using analytical gradient procedures,[34] employing DFT calculations. The spin-unrestricted version of the Becke three-parameter hybrid functional[35] combined with the Lee, Yang, and Parr correlation functional,[36] denoted as UB3LYP,[37] was employed with the split-valence 6-31G(d) basis set.[38] All of the stationary points were characterized by their harmonic vibrational frequencies as minima or saddle points. Connections of the transition-state structures between designated minima were confirmed in each case by intrinsic reaction coordinate (IRC)[39] calculations using the second-order algorithm of Gonzalez and Schlegel.[40]

We investigated the effect of adding diffuse sp functions[41] on heavy atoms to the 6-31G(d) basis set on the optimized geometries of the stationary points located at the UB3LYP/6-31G(d) level. The geometries of the reactants (**1** and O_2), five transition structures, and four reaction products involved in reaction pathways shown in Schemes 2 and 3 were obtained with the 6-31G(d) and 6-31+G(d) basis sets and resulted not to differ significantly. Next, the geometries optimized with both basis sets for the reactants and the five transition structures were used in single-point energy calculations at ab initio high levels of theory (see below). The relative energy differences were found to be at variance by 0.5 kcal/mol at most. Furthermore, because the **1** + O_2 reaction system involves two unpaired electrons in O_2 interacting with five delocalized electrons in the π system of radical **1**, we also investigated the effect on the optimized geometries of the transition structures located with the UB3LYP functional of the multireference character expected for these structures. To this end, the geometries of the reactants (**1** and O_2) and five transition structures involved in reaction pathways shown in Schemes 2 and 4 were reoptimized by use of a multiconfiguration self-consistent field wave function of the complete active space (CASSCF) class[42] with the 6-31G(d) basis set. The CAS consisted of 13 electrons and 11 orbitals: the five electrons and five orbitals involved in the π system of the radical **1** unit plus eight electrons and six orbitals of the O_2 unit. The CASSCF-optimized geometries were found to be consistent with those obtained using the B3LYP functional. Details on the two tests are given in the Supporting Information (see Table S1 and Figures S1 and S2). Therefore, the procedure of using the UB3LYP/6-31G(d)-optimized structures in the final single-point calculations at ab initio high levels of theory was deemed safe and adopted throughout this study.

It is well-known that the energy barriers affect the calculated rate coefficients exponentially. Hence, it is crucial to compute accurately the energies of the transition-state structures relative to those of the reactants. Because it is notorious that the UB3LYP functional underestimates the energy barriers calculated for some radical reactions (e.g., in the case of loose transition states and H-atom abstraction reactions),[43] we carried out single-point (frozen core) coupled-

Scheme 5

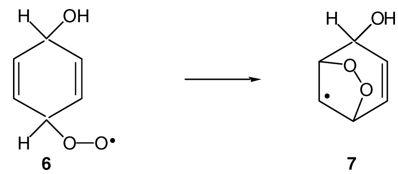

cluster[44] calculations including all single and double excitations, based on a reference unrestricted Hartree−Fock (UHF) single determinant, together with a perturbative treatment of all connected triple excitations,[45] designated by UCCSD(T), with the 6-311+G(2df,2p) basis set[46] using the geometries optimized at the UB3LYP/6-31G(d) level. A special difficulty is encountered in the case of the transition-state structures located for the competing reactions shown in Schemes 2−5 because we found a significant difference in the degree of spin contamination shown by the UHF wave function underlying the UCCSD(T) calculations. In fact, the expected values of the spin-squared operator for the UHF/6-311+G(2df,2p) wave function (designated by $\langle S^2 \rangle$) of the transition-state structures calculated for these reactions were ranging between 1.14 and 2.19 (see Table S3, Supporting Information). Therefore, all of the energies were refined by performing single-point energy calculations on the UB3LYP geometries using (frozen core) partially spin-adapted CCSD(T) calculations based on a restricted open-shell Hartree−Fock (ROHF) reference single determinant,[47] designated by RCCSD(T), to avoid the spin contamination problem of the UCCSD(T) calculations.[48]

As noted above, some of the transition states involved in the **1** + O_2 reaction system may have appreciable multireference character and, therefore, may not be well treated with a single-reference based method such as RCCSD(T). To test this suspicion, we computed the T_1 diagnostic values at the RCCSD/6-311+G(2df,2p) level, based on the open-shell formalism of Jayatilaka and Lee,[49] for all of the open-shell species considered in this study (see Table S3, Supporting Information). The T_1 diagnostic gives a qualitative assessment of the significance of nondynamical electron correlation: the larger is the T_1 diagnostic value, the less reliable are the results of the single-reference coupled cluster wave function. For example, the RCCSD method is considered somewhat less reliable if the T_1 diagnostic value is larger than 0.044.[43,50] Examining Table S3 (Supporting Information), we see that all species have T_1 diagnostic values ranging between 0.015 and 0.040 except the transition structure **TS1′**. Thus, our computed RCCSD(T) energy results for **TS1′** may not be entirely reliable, although surely not unreasonable. Fortunately, the energy of **TS1′** is of lesser importance to this study. It is clear then that for all species except **TS1′** our RCCSD(T) results should be reasonably reliable. To provide additional support to this assertion, single-point second-order multiconfigurational perturbation theory calculations (CASPT2),[51] based on the CASSCF(13,11) reference function, were carried out with the 6-31G(d) basis set for the reactants (**1** and O_2) and five transition structures relevant to reactions shown in Schemes 2 and 4. The CASSCF(13,11)/6-31G(d)-optimized geometries were used in these CASPT2 calculations. As shown in Table S2 (Supporting Information), the relative energy orderings of these transition structures determined from the CASPT2/6-31G(d) and RCCSD(T)/6-311+G(2df,2p) calculations compare reasonably well.

Zero-point vibrational energies (ZPVEs) were determined from unscaled harmonic vibrational frequencies. Thermal corrections to enthalpy and Gibbs energy values were obtained assuming ideal gas behavior from the unscaled harmonic frequencies and moments of inertia by conventional methods.[52] A standard pressure of 1 atm was taken in the absolute entropy calculations.

All of the UB3LYP and UCCSD(T) calculations were carried out by using the Gaussian 03 program package,[53] whereas the MOLPRO 98 program package[54] was employed for the RCCSD(T) and T_1 diagnostic computations. The CASSCF and CASPT2 calculations were performed by using the GAMESS[55] and MOLCAS-6[56] program packages, respectively.

2.2. Rate Coefficient and Equilibrium Constant Calculations. It is well-known that the theoretical rate coefficient of a reaction is extremely sensitive to the value of the reaction energy barrier. For instance, a change of only 1.4 kcal/mol on the calculated energy barrier causes a change of about a factor of 10 on the calculated rate coefficient.[22] With the main purpose of ascertaining the reliability of the energy barriers obtained from both the UCCSD(T) and the RCCSD(T) calculations, the rate coefficient, k, of the competing reactions shown in Schemes 2−5 was evaluated by using the conventional transition-state theory equation:[57]

$$k = \Gamma \frac{k_b T}{h} \frac{Q_{TS}}{Q_R} e^{-(E_{TS}-E_R)/RT} \tag{1}$$

where Q_{TS} is the partition function of the transition state; Q_R is the product of the partition functions of the reactants; E_{TS} and E_R are the total energy plus the ZPVE of the transition state and reactants, respectively; k_b is the Boltzmann constant; R is the ideal gas constant; T is the absolute temperature; and Γ is the tunneling factor.

According to the standard formulas,[52] the Q's were evaluated using the UB3LYP/6-31(d) geometries and harmonic vibrational frequencies, while the E's were taken as the ZPVE-corrected UCCSD(T)/6-311+G(2df,2p) and RCCSD(T)/6-311+G(2df,2p) energies. The Γ's were evaluated by zero-order approximation to the vibrationally adiabatic PES model with zero curvature.[58] In this approximation, the tunneling is assumed to occur along a unidimensional minimum energy path. The potential energy curve is approximated by an unsymmetrical Eckart potential energy barrier[59] that is required to go through the ZPVE corrected energy (denoted as E) of the reactants, transition state, and products. The equations that describe the Eckart potential energy function were adapted from Truong and Truhlar.[58] Solving the Schroedinger equation for the Eckart function yields the transmission probability, $\kappa(E)$. Γ is then obtained by integrating the respective $\kappa(E)$ over all possible energies:

$$\Gamma(T) = \frac{1}{k_b T} e^{(E_{TS}-E_R)/k_b T} \int_0^\infty e^{-E/k_b T} \kappa(E)\, dE \tag{2}$$

For the reactions of radical **1** with O_2 leading to the formation of peroxyl radicals **4** and **6**, the equilibrium constants expressed in concentration units (denoted as K_c) were evaluated by using the standard formulas:[60]

$$K_c = K_p R'T \tag{3}$$

$$RT \ln K_p = -\Delta G_T^0 \tag{4}$$

where R' is the ideal gas constant in liter atmosphere units, that is, 0.082 L atm/(mol·K), K_p is the equilibrium constant expressed in pressure units, and $\Delta G_T{}^0$ is the standard Gibbs energy change at 1 atm.

3. Results and Discussion

Selected geometrical parameters of the most relevant structures concerning the stationary points located on the ground-state PES of the **1** + O_2 reaction system at the UB3LYP/6-31G(d) level are shown in Figures 1−6. The Cartesian coordinates of all structures reported in this Article are available as Supporting Information. Total energies computed at UB3LYP, UCCSD(T), and RCCSD(T) levels of theory using the UB3LYP/6-31G(d)-optimized geometries, as well as the ZPVEs, thermal corrections to enthalpy, and Gibbs energy, for all structures are collected in Table S4 (Supporting Information). Tables 1−5 give the relative energies (ΔU), calculated at the UB3LYP, RCCSD(T), and UCCSD(T) levels, the relative energies at 0 K (ΔE(0 K)), and the relative enthalpies (ΔH(298 K)) and Gibbs energies (ΔG(298 K)) at 298 K, calculated at the RCCSD(T) and UCCSD(T) levels, for the stationary points involved in each reaction pathway considered in the present study. Figures 7 and 8 display schematic Gibbs energy profiles of the relevant reaction pathways concerning the O_2 addition to positions 2 and 4 of the benzene ring in radical **1** and the subsequent ring closure of the peroxyl radicals formed. Finally, the values of Γ and k at 298 K for the bimolecular and unimolecular reactions are summarized in Tables 6 and 7, respectively.

3.1. H-Atom Abstraction by O_2 in Hydroxycyclohexadienyl Radical Affording Phenol. Table 1 gives the values of ΔU, ΔE(0 K), ΔH(298 K), and ΔG(298 K) calculated at different levels of theory for the relevant stationary points for the reaction pathway **A** in Scheme 2. In agreement with earlier UB3LYP/6-31(+)G(d) calculations by Ghigo and Tonachini,[26] we found two transition structures for this reaction channel (labeled as **TS1** and **TS1′** in Figure 1). Their geometries differ one from the other essentially in the orientation of the O−O and O−H bonds relative to the benzene cycle. Furthermore, **TS1′** shows an intermolecular hydrogen bond between an oxygen atom of the O_2 unit and the hydrogen atom of the OH group. However, the UB3LYP/6-31G(d) calculations predict that the total energy of **TS1′** is 1.4 kcal/mol higher than that of **TS1** (see Table 1). To investigate the origin of this unexpected result, we performed an analysis of the electron density in **TS1** and **TS1′** within the framework of the topological theory of an atoms in molecules (AIM).[61] The AIM topological analysis of the electron density in **TS1′** revealed the presence of a bond critical point between one of the two oxygen atoms of the O_2 unit and the hydrogen atom of the OH group, with an electron density of 0.0289 e, which can be associated with the aforementioned intermolecular

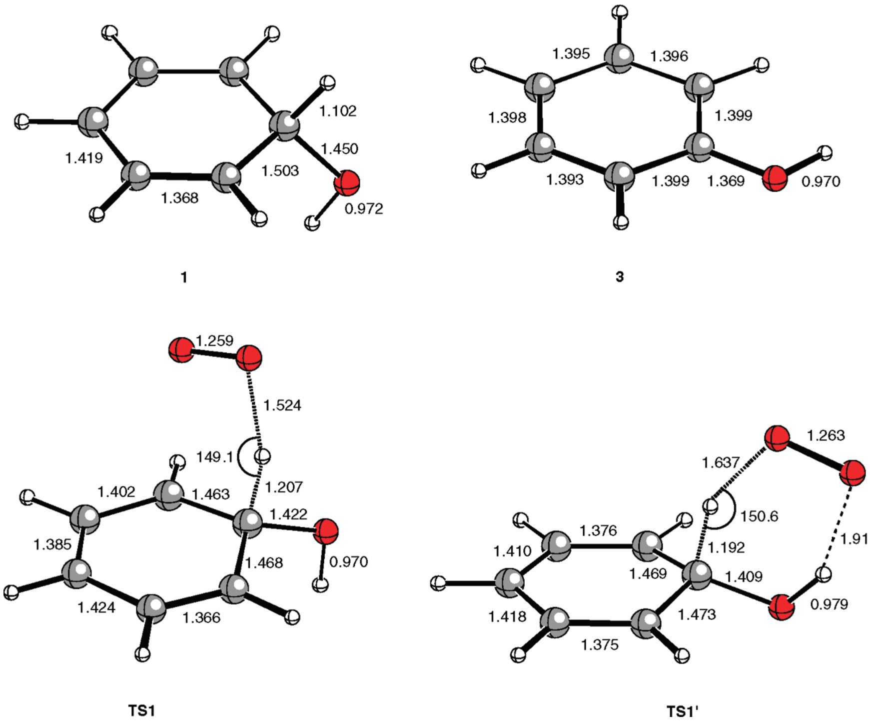

Figure 1. Selected geometrical parameters of the equilibrium structures of hydroxycyclohexadienyl radical (**1**), phenol (**3**), and the transition structures for the H-atom abstraction by O_2 in **1** affording **3**. Distances are given in angstroms and angles are in degrees.

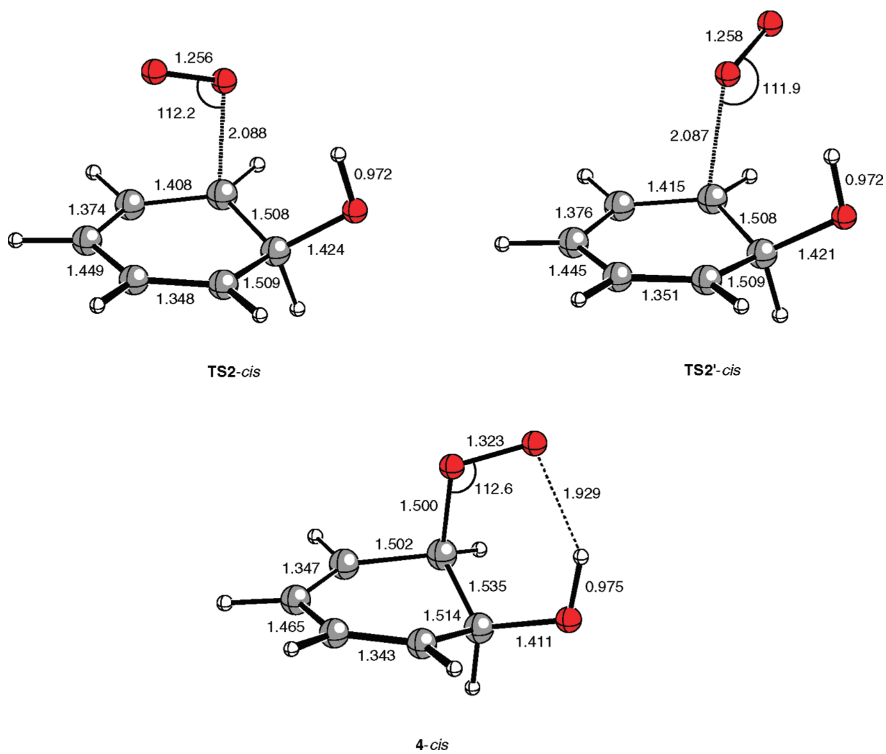

Figure 2. Selected geometrical parameters of the transition structures (**TS2**-*cis* and **TS2′**-*cis*) for the O_2 addition to position 2 of the benzene ring in radical **1** and the equilibrium structure (**4**-*cis*) of the cis stereoisomer of peroxyl radical **4**. Distances are given in angstroms and angles are in degrees.

hydrogen bond between these atoms. On the other hand, the AIM topological analysis of the electron density in **TS1** showed the presence of a bond critical point between one of the two oxygen atoms of the O_2 unit and the closer carbon atom at position 2 of the benzene ring, with an electron density of 0.0363 e. Therefore, although **TS1** does not show any hydrogen-bonding interaction, in this transition structure there exists an extra binding interaction between the O_2 molecule and the radical **1**, which is lacking in **TS1′**. Thus, the lower energy of **TS1** might be ascribed to the larger value of the electron density

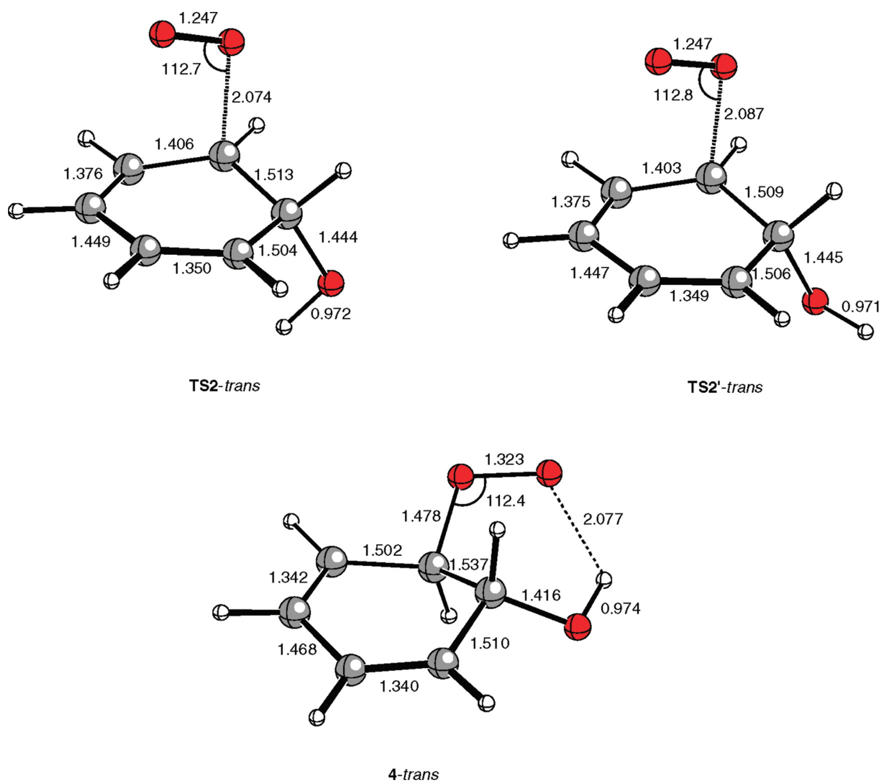

Figure 3. Selected geometrical parameters of the transition structures (**TS2**-*trans* and **TS2′**-*trans*) for the O_2 addition to position 2 of the benzene ring in radical **1** and the equilibrium structure (**4**-*trans*) of the trans stereoisomer of peroxyl radical **4**. Distances are given in angstroms and angles are in degrees.

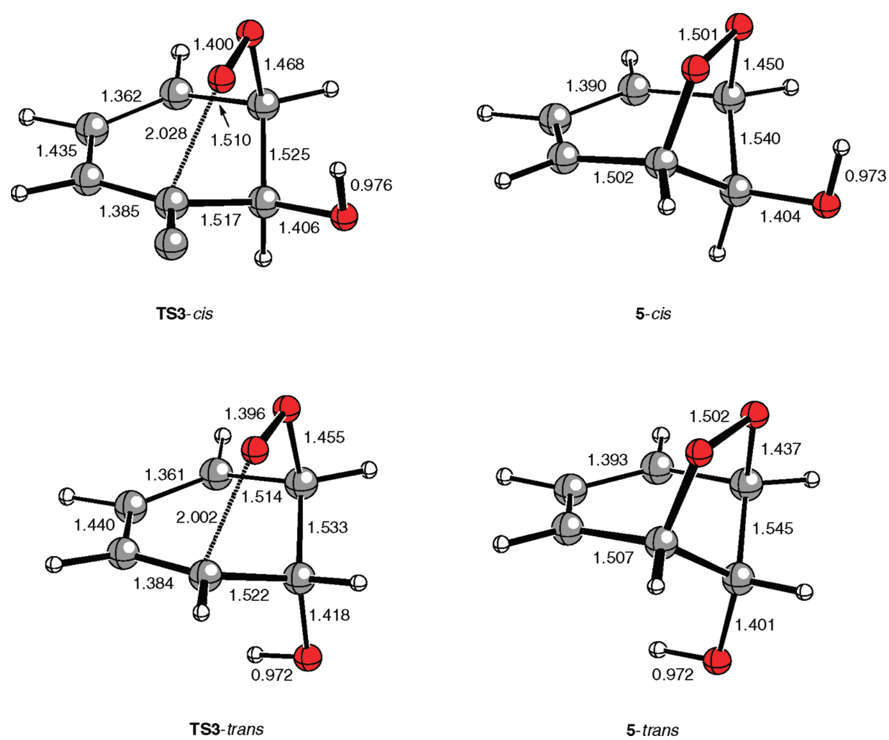

Figure 4. Selected geometrical parameters of the transition structures (**TS3**-*cis* and **TS3**-*trans*) for the cyclization of radicals **4**-*cis* and **4**-*trans* to bicyclic allyl radical **5** and the equilibrium structures (**5**-*cis* and **5**-*trans*) of the cis and trans stereoisomers of this radical. Distances are given in angstroms.

calculated at the bond critical point associated with the latter binding interaction in **TS1**, as compared to that calculated at the bond critical point associated with the hydrogen-bonding interaction in **TS1′**.

At the UCCSD(T) and RCCSD(T) levels, the energy difference between **TS1** and **TS1′** increases to the values of 3.0 and 5.9 kcal/mol, respectively. The $\langle S^2 \rangle$ values calculated for the UHF/6-311+G(2df,2p) wave function of **TS1** and

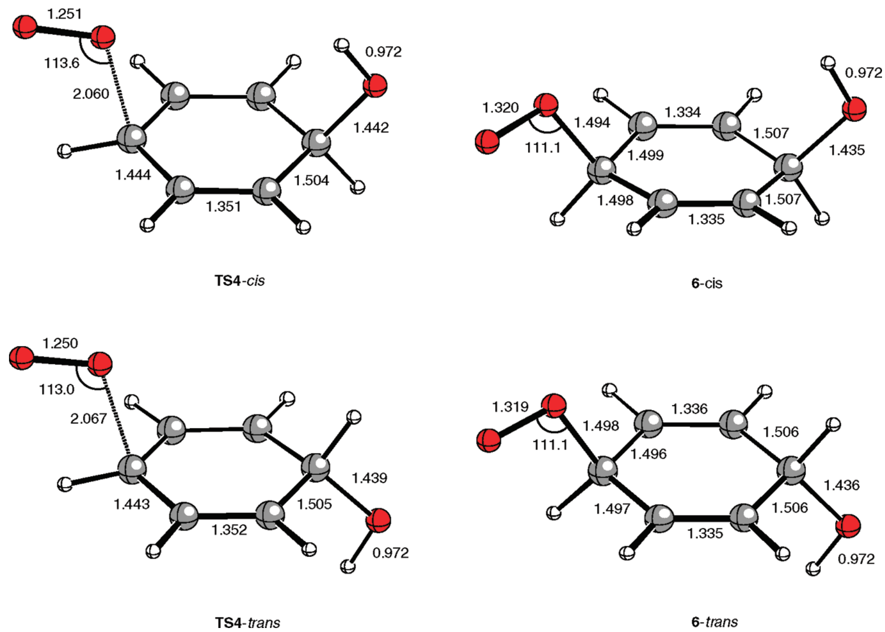

Figure 5. Selected geometrical parameters of the transition structures (**TS4**-*cis* and **TS4**-*trans*) for the O_2 addition to position 4 of the benzene ring in radical **1** and the equilibrium structures (**6**-*cis* and **6**-*trans*) of the cis and trans stereoisomers of peroxyl radical **6**. Distances are given in angstroms and angles are in degrees.

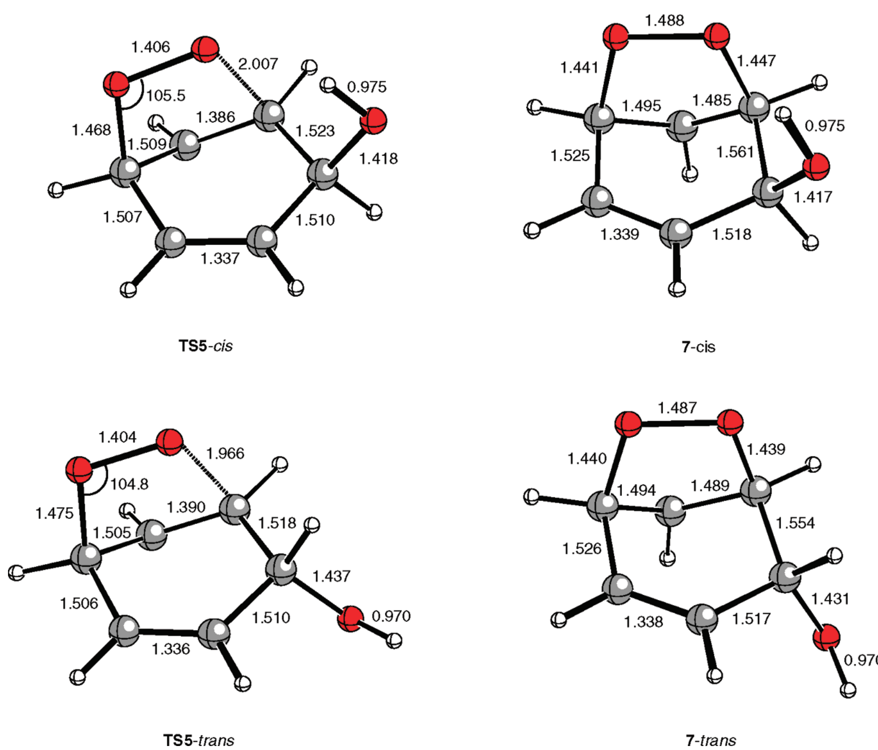

Figure 6. Selected geometrical parameters of the transition structures (**TS5**-*cis* and **TS5**-*trans*) for the cyclization of radicals **6**-*cis* and **6**-*trans* to bicyclic allyl radical **7** and the equilibrium structures (**7**-*cis* and **7**-*trans*) of the cis and trans stereoisomers of this radical. Distances are given in angstroms and angles are in degrees.

TS1′ are 2.08 and 2.19, respectively. As a consequence, the heights of the barriers computed with the UCCSD(T) and RCCSD(T) methods should differ significantly. In fact, focusing on the lowest energy transition structure **TS1**, the energy barrier in terms of ΔU (designated by $\Delta U^{\ddagger}$) calculated with these methods is 11.8 and 4.7 kcal/mol, respectively (see Table 1). The energy barrier calculated at the RCCSD(T) level leads to a rate coefficient at 298 K of 4.2×10^{-18} molecule^{-1} cm^3 s^{-1} (see Table 6), which is a factor of about 10 lower than the estimated experimental[22] value of $(6-11) \times 10^{-17}$ molecule^{-1} cm^3 s^{-1}. On the other hand, the energy barrier calculated at the UCCSD(T) level leads to a rate coefficient at 298 K of 3.1×10^{-23} molecule^{-1} cm^3 s^{-1}, which is too low by a factor of 10^6 as compared to the estimated experimental result. Therefore, it appears that the RCCSD(T) method performs much better than UCCSD(T) in the calculation of the energy barrier for H-atom abstraction from **1** by O_2 affording phenol. This finding is consistent

Table 1. Relative Energies (kcal/mol) of the Most Relevant Stationary Points on the Ground-State Potential Energy Surface for H-Atom Abstraction by O_2 in Hydroxycyclohexadienyl Radical (**1**) Forming Phenol (**3**)

	UB3LYP[a]	RCCSD(T)[b]			
stationary point[c]	ΔU	ΔU	ΔE(0 K)	ΔH(298 K)	ΔG(298 K)
1 + O_2	0.0	0.0	0.0	0.0	0.0
TS1	3.0	4.7 (11.8)	4.5 (11.5)	3.7 (10.8)	14.7 (21.8)
TS1′	4.4	10.6 (14.8)	9.8 (14.0)	9.2 (13.4)	19.3 (23.5)
3 + HOO$^•$	−26.2	−29.9 (−30.3)	−29.2 (−29.6)	−29.3 (−30.9)	−29.6 (−30.0)

[a] Calculated with the 6-31G(d) basis set. [b] Calculated with the 6-311+G(2df,2p) basis set. The values calculated at the UCCSD(T) level with the same basis set are given in parentheses. [c] See Figure 1.

Table 2. Relative Energies (kcal/mol) of the Most Relevant Stationary Points on the Ground-State Potential Energy Surface for O_2 Addition to Position 2 of Benzene Ring in Hydroxycyclohexadienyl Radical (**1**)

	UB3LYP[a]	RCCSD(T)[b]			
stationary point[c]	ΔU	ΔU	ΔE(0 K)	ΔH(298 K)	ΔG(298 K)
1 + O_2	0.0	0.0	0.0	0.0	0.0
TS2-*cis*	2.3	1.5 (6.6)	3.3 (8.4)	2.5 (7.6)	13.9 (19.0)
TS2′-*cis*	4.8	7.0 (10.8)	8.1 (12.0)	7.5 (11.4)	18.0 (21.8)
4-*cis*	−8.3	−12.7 (−13.4)	−9.4 (−10.1)	−10.3 (−11.0)	1.4 (0.7)
TS2-*trans*	3.1	1.5 (6.4)	3.2 (8.1)	2.5 (7.4)	13.6 (18.4)
TS2′-*trans*	5.9	3.9 (8.8)	5.2 (10.1)	4.7 (9.6)	15.3 (20.2)
4-*trans*	−9.4	−14.0 (−14.7)	−10.6 (−11.3)	−11.5 (−12.2)	0.0 (−0.7)

[a] Calculated with the 6-31G(d) basis set. [b] Calculated with the 6-311+G(2df,2p) basis set. The values calculated at the UCCSD(T) level with the same basis set are given in parentheses. [c] See Figures 2 and 3.

Table 3. Relative Energies (kcal/mol) of the Most Relevant Stationary Points on the Ground-State Potential Energy Surface for the Cyclization of Peroxyl Radical **4** to the Bicyclic Allyl Radical **5**

	UB3LYP[a]	RCCSD(T)[b]			
stationary point[c]	ΔU	ΔU	ΔE(0 K)	ΔH(298 K)	ΔG(298 K)
4-*cis*	0.0	0.0	0.0	0.0	0.0
TS3-*cis*	10.6	13.4 (13.6)	13.1 (13.3)	12.4 (12.7)	14.1 (14.3)
5-*cis*	−8.1	−11.7 (−10.8)	−11.4 (−10.5)	−11.9 (−11.0)	−10.6 (−9.7)
4-*trans*	0.0	0.0	0.0	0.0	0.0
TS3-*trans*	17.1	18.8 (19.4)	18.4 (19.0)	17.9 (18.5)	19.5 (20.0)
5-*trans*	−3.8	−7.0 (−6.2)	−6.7 (−5.9)	−7.2 (−6.4)	−5.7 (−4.9)

[a] Calculated with the 6-31G(d) basis set. [b] Calculated with the 6-311+G(2df,2p) basis set. The values calculated at the UCCSD(T) level with the same basis set are given in parentheses. [c] See Figures 2−4.

Table 4. Relative Energies (kcal/mol) of the Most Relevant Stationary Points on the Ground-State Potential Energy Surface for O_2 Addition to Position 4 of Benzene Ring in Hydroxycyclohexadienyl Radical (**1**)

	UB3LYP[a]	RCCSD(T)[b]			
stationary point[c]	ΔU	ΔU	ΔE(0 K)	ΔH(298 K)	ΔG(298 K)
1 + O_2	0.0	0.0	0.0	0.0	0.0
TS4-*cis*	4.2	4.6 (8.1)	6.0 (9.5)	5.5 (9.0)	15.2 (18.7)
6-*cis*	−8.3	−12.4 (−13.0)	−9.0 (−9.6)	−9.8 (−10.4)	1.0 (0.4)
TS4-*trans*	4.0	4.8 (8.2)	6.1 (9.6)	5.7 (9.1)	15.5 (18.9)
6-*trans*	−7.0	−12.3 (−12.9)	−9.0 (−9.6)	−11.7 (−12.3)	−0.9 (−1.5)

[a] Calculated with the 6-31G(d) basis set. [b] Calculated with the 6-311+G(2df,2p) basis set. The values calculated at the UCCSD(T) level with the same basis set are given in parentheses. [c] See Figure 5.

with the fact that spin contamination is eliminated in the RCCSD(T) calculation of $\Delta U^{\ddagger}$.

We note that the values (1.18 and 1.19) of the tunneling factor Γ obtained with the RCCSD(T) and UCCSD(T) methods for the phenol channel (see Table 6) indicate that the tunneling effect in this reaction is negligible. This feature is contrary to common belief that for an H-atom transfer process the tunneling effect should be important. This unexpected result is ascribed to the fact that the energy barriers of reaction pathway **A** in Scheme 2 are broad, as suggested by the small value (415.9i cm^{-1}) of the imaginary vibrational frequency of the transition structure **TS1**.

To compare the results of our computations for the phenol channel with those of Lesclaux and co-workers,[22] it is convenient to consider the calculated enthalpy of activation at 298 K (designated by $\Delta H^{\ddagger}$(298 K)). By using a combination of UB3LYP/6-31G(d) and UCCSD(T)/6-31G(d,p) computations with an empirical relationship between $\Delta H^{\ddagger}$(298 K) and the reaction enthalpy at 298 K (designated by ΔH_r(298 K)), Lesclaux and co-workers[22] determined a $\Delta H^{\ddagger}$(298 K) of 1.8 kcal/mol. This value leads to a rate coefficient at 298 K of 1.4 × 10^{-16} $molecule^{-1}$ cm^3 s^{-1}, which is in good agreement with the estimated experimental value. On the other hand, the RCCSD(T)/6-311+G(2df,2p)

Table 5. Relative Energies (kcal/mol) of the Most Relevant Stationary Points on the Ground-State Potential Energy Surface for the Cyclization of Peroxyl Radical **6** to the Bicyclic Allyl Radical **7**

	UB3LYP[a]	RCCSD(T)[b]			
stationary point[c]	Δ*U*	Δ*U*	Δ*E*(0 K)	Δ*H*(298 K)	Δ*G*(298 K)
6-*cis*	0.0	0.0	0.0	0.0	0.0
TS5-*cis*	30.3	30.7 (31.6)	29.9 (30.7)	29.1 (29.8)	31.6 (32.4)
7-*cis*	11.0	7.6 (8.1)	7.8 (8.3)	7.1 (7.6)	9.4 (9.9)
6-*trans*	0.0	0.0	0.0	0.0	0.0
TS5-*trans*	35.4	34.2 (34.9)	32.7 (33.5)	34.2 (35.0)	36.0 (36.7)
7-*trans*	15.5	10.8 (11.4)	10.6 (11.2)	12.0 (12.6)	13.8 (14.4)

[a] Calculated with the 6-31G(d) basis set. [b] Calculated with the 6-311+G(2df,2p) basis set. The values calculated at the UCCSD(T) level with the same basis set are given in parentheses. [c] See Figures 5 and 6.

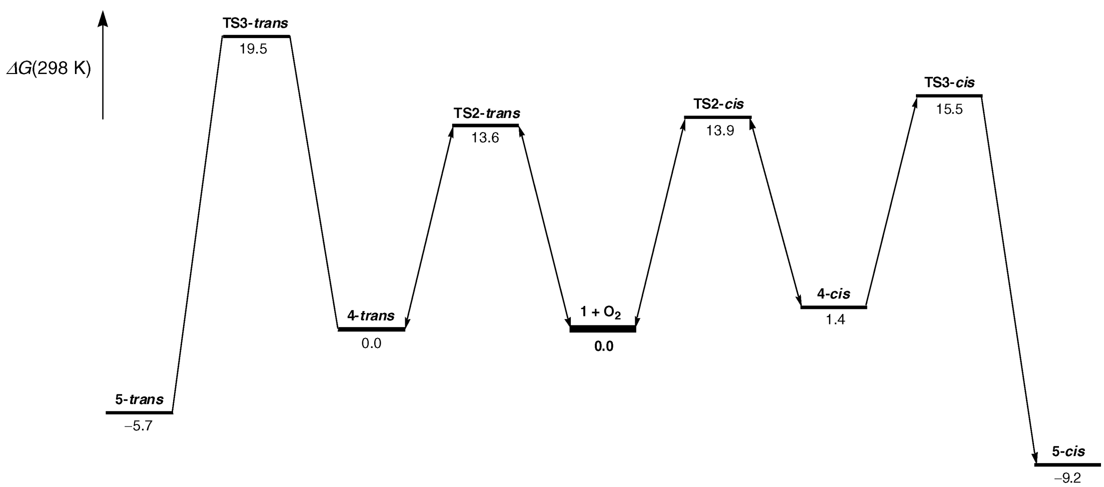

Figure 7. Schematic Gibbs energy profiles of the relevant reaction pathways concerning the O_2 addition to position 2 of the benzene ring in radical **1** and the subsequent ring closure of the peroxyl radicals **4**-*cis* and **4**-*trans*. Relative Gibbs energy values at 298 K (Δ*G*(298 K)) determined from RCCSD(T)/6-311+G(2df,2p) calculations.

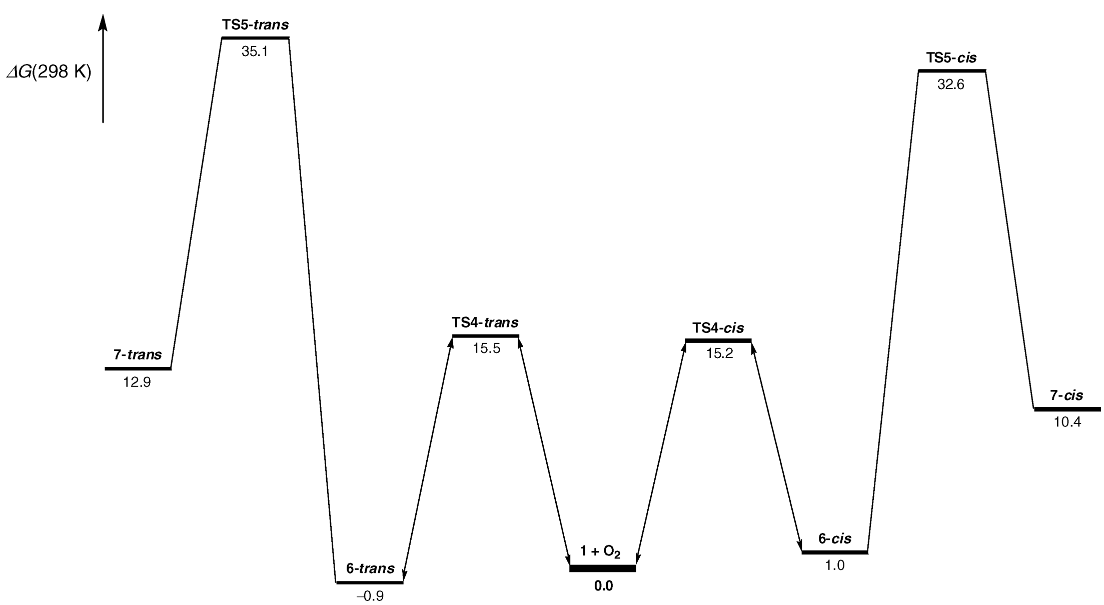

Figure 8. Schematic Gibbs energy profiles of the relevant reaction pathways concerning the O_2 addition to positions 4 of the benzene ring in radical **1** and the subsequent ring closure of the peroxyl radicals **6**-*cis* and **6**-*trans*. Relative Gibbs energy values at 298 K (Δ*G*(298 K)) determined from RCCSD(T)/6-311+G(2df,2p) calculations.

calculations predicts a $\Delta H^{\ddagger}$(298 K) of 3.7 kcal/mol (see Table 1), which is 1.9 kcal/mol higher than the value obtained by Lesclaux and co-workers and leads to a rate coefficient at 298 K that is a factor of about 10 lower than the estimated experimental value. Therefore, one might think that the semiempirical procedure of Lesclaux and co-workers performs much better than our approach, based on RCCSD(T)/6-311+G(2df,2p) calculations, in predicting activation energy barriers. However, our approach has the advantage of avoiding the use of empirical relationships between $\Delta H^{\ddagger}(T)$

Table 6. Tunneling Factor (Γ; See eq 2) and Rate Coefficient (k in molecule^{-1} cm^3 s^{-1}; See eq 1) at 298 K Calculated for Bimolecular Reactions Forming Phenol (**3**) and Peroxyl Radicals **4** and **6**[a]

reaction	TS	Γ	k
1 + O_2 → **3** + HOO$^•$	**TS1**	1.18 (1.19)	4.2×10^{-18} (3.1×10^{-23})
1 + O_2 → **4**-*cis*	**TS2**-*cis*	1.19 (1.12)	1.9×10^{-17} (3.4×10^{-21})
1 + O_2 → **4**-*trans*	**TS2**-*trans*	1.19 (1.12)	3.2×10^{-17} (9.2×10^{-21})
1 + O_2 → **6**-*cis*	**TS4**-*cis*	1.17 (1.15)	2.1×10^{-18} (5.7×10^{-21})
1 + O_2 → **6**-*trans*	**TS4**-*trans*	1.16 (1.15)	1.3×10^{-18} (4.0×10^{-21})

[a] Calculated at the RCCSD(T) level of theory with the 6-311+G(2df,2p) basis set. The values calculated at the UCCSD(T) level with the same basis set are given in parentheses.

Table 7. Tunneling Factor (Γ; See eq 2) and Rate Coefficient (k in s^{-1}; See eq 1) at 298 K Calculated for Unimolecular Reactions of Cyclization of Peroxyl Radicals **4** and **6** and Their Reversible Decomposition Back to **1** + O_2[a]

reaction	TS	Γ	k
4-*cis* → **5**-*cis*	**TS3**-*cis*	1.26 (1.12)	3.6×10^{2} (2.6×10^{2})
4-*cis* → **1** + O_2	**TS3**-*cis*	1.19 (1.12)	5.1×10^{3} (2.7×10^{-1})
4-*trans* → **5**-*trans*	**TS3**-*trans*	1.31 (1.31)	4.1×10^{-2} (1.8×10^{-2})
4-*trans* → **1** + O_2	**TS3**-*trans*	1.19 (1.12)	7.9×10^{2} (7.0×10^{-2})
6-*cis* → **7**-*cis*	**TS5**-*cis*	1.79 (1.80)	7.7×10^{-11} (2.0×10^{-11})
6-*cis* → **1** + O_2	**TS5**-*cis*	1.17 (1.15)	2.8×10^{2} (2.8×10^{-1})
6-*trans* → **7**-*trans*	**TS5**-*trans*	1.91 (1.92)	4.9×10^{-14} (1.5×10^{-14})
6-*trans* → **1** + O_2	**TS5**-*trans*	1.16 (1.159)	6.8×10^{1} (7.9×10^{-3})

[a] Calculated at the RCCSD(T) level of theory with the 6-311+G(2df,2p) basis set. The values calculated at the UCCSD(T) level with the same basis set are given in parentheses.

and $\Delta H_r(T)$. Furthermore, as shown below, the relative energy barriers determined at the RCCSD(T) level of theory with the 6-311+G(2df,2p) basis set for the competing reactions arising from the reaction **1** + O_2 turn out to be reasonably reliable.

Regarding the ΔH_r(298 K) of the phenol channel (see Table 1), it is to be noted that the value of −30.9 kcal/mol calculated with the UCCSD(T) method using the 6-311+G(2df,2p) basis set is 4.4 kcal/mol more negative than the value of −26.5 kcal/mol calculated with the same method using the 6-31G(d,p) basis set, reported by Lesclaux and co-workers.[22] It turns out, therefore, that the ΔH_r(298 K) calculated for the reaction channel affording phenol depends significantly on the size of the basis set employed. Furthermore, there is a difference of 1.6 kcal/mol between the values of ΔH_r(298 K) calculated with the UCCSD(T) and RCCSD(T) methods using the 6-311+G(2df,2p) basis set. This feature is ascribed to the significant spin contamination in the UHF/6-311+G(2df,2p) wave function of **1** (i.e., $\langle S^2 \rangle = 1.17$).

Earlier energy calculations by Ghigo and Tonachini[23,26] concerning the phenol channel, performed at the single-point UB3LYP/6-311+G(d,p) level using UB3LYP/6-31(+)G(d)-optimized geometries with energies corrected for spin contamination, are in reasonable agreement with the results of our RCCSD(T) calculations. Both the energy barrier and the energy of reaction in terms of ΔG(298 K) reported by Ghigo and Tonachini[23] (i.e., 13.6 and −27.6 kcal/mol, respectively) compare fairly well with our values of 14.7 and −29.6 kcal/mol, obtained at the RCCSD(T)/6-311+G(2df,2p) level.

3.2. O_2 Addition to Position 2 of the Benzene Ring in Hydroxycyclohexadienyl Radical. Table 2 gives the values of ΔU, ΔE(0 K), ΔH(298 K), and ΔG(298 K) calculated at different levels of theory for the relevant stationary points of the reaction pathway B in Scheme 2. In agreement with the results of earlier theoretical studies,[20,22] we found that the lowest energy structure of both the cis and the trans stereoisomers of peroxyl radical **4** (labeled as **4**-*cis* and **4**-*trans* in Figures 2 and 3, respectively) shows an intramolecular hydrogen bond between the terminal oxygen atom of the O−O fragment and the H-atom of the OH group. The lowest energy isomer corresponds to **4**-*trans*, whose ΔH(298 K) calculated at either the UCCSD(T) or the RCCSD(T) level of theory is 1.2 kcal/mol lower than that of **4**-*cis*. The ΔH_r(298 K) values determined with the UCCSD(T) method for the reactions affording **4**-*cis* and **4**-*trans* (i.e., −11.0 and −12.2 kcal/mol, respectively) are 0.7 kcal/mol more negative than those calculated with the RCCSD(T) (i.e., −10.3 and −11.5 kcal/mol, respectively). Lesclaux and co-workers[22] have reported an experimental ΔH_r(298 K) value of −12.5 kcal/mol for the O_2 addition to position 2 of the benzene ring in **1** affording peroxyl radical **4**. This value was determined from the measured thermodynamic equilibrium constant at 295 K for this reaction, assuming that the observed equilibrium must essentially involve the trans isomer of **4**, by using a reaction entropy at 298 K of −38.6 cal/mol·K (obtained from the UB3LYP/6-31G(d) calculations). At this point, we note that Lesclaux and co-workers assume that the chemical equilibrium **1** + O_2 ↔ **4** essentially involves the trans isomer of **4** on the basis of theoretical calculations predicting that the cis isomer is energetically less stable than the trans one and that its formation rate is significantly slower. However, it is not possible to resolve these isomers on the basis of the currently available experimental data. In the processing of the temperature-dependent equilibrium constants experimental data, it was assumed a single isomer of radical **4**, hence not differentiating the cis and trans isomers.[22]

The equilibrium between formation and decomposition of the peroxyl radicals **4**-*cis* and **4**-*trans* was evaluated according to eqs 3 and 4. The equilibrium constants at 298 K predicted by the RCCSD(T) and UCCSD(T) methods are given in Table 8. The equilibrium constant of reaction pathway **B** in Scheme 2 has been measured in several experimental studies.[18,20–22] Bohn and Zetzsch[18] determined an equilibrium constant of 2.7×10^{-19} cm^3 molecule^{-1} at 298 K, whereas Lesclaux and co-workers reported a value of 1.15×10^{-19} cm^3 molecule^{-1} at 295 K. More recently,

Table 8. Standard Gibbs Energy Change at 1 atm and 298 K ($\Delta G°$ in kcal mol^{-1}) and Equilibrium Constants (K_c in molecule^{-1} cm^3) at 298 K Calculated for the Reactions Forming Peroxyl Radicals **4** and **6**

reaction	RCCSD(T)[a] $\Delta G°$	RCCSD(T)[a] K_c	UCCSD(T)[b] $\Delta G°$	UCCSD(T)[b] K_c
1 + O_2 ↔ **4**-*cis*	1.4	3.82×10^{-21}	0.7	1.25×10^{-20}
1 + O_2 ↔ **4**-*trans*	0.0	4.06×10^{-20}	−0.7	1.32×10^{-19}
1 + O_2 ↔ **6**-*cis*	1.0	7.51×10^{-21}	0.4	2.07×10^{-20}
1 + O_2 ↔ **6**-*trans*	−0.9	1.86×10^{-19}	−1.5	5.11×10^{-19}

[a] Determined from relative energies calculated at the RCCSD(T) level of theory with the 6-311+G(2df,2p) basis set. [b] Determined from relative energies calculated at the UCCSD(T) level of theory with the 6-311+G(2df,2p) basis set.

the latter authors measured a value of $(2.62 \pm 0.24) \times 10^{-19}$ cm^3 molecule^{-1} at 295 K, which is in good agreement with that reported by Bohn and Zetzsch. Table 8 shows that the equilibrium constants for **4**-*cis* and **4**-*trans* obtained from the RCCSD(T) calculations are about a factor of 71 and 7, respectively, lower than the experimental value reported by Bohn and Zetzsch.[18] Interestingly, the values determined from the UCCSD(T) calculations for **4**-*cis* and **4**-*trans* are about a factor of 22 and 2, respectively, lower than the latter experimental value. These results suggest that the values of ΔH_r(298 K) predicted by the UCCSD(T) method are more reliable than those predicted by RCCSD(T) method. However, it should be stressed again that the experiments performed in all of these studies could not distinguish between the possible isomers of peroxyl radical **4**. This fact should be taken into account when comparing the experimental results with the theoretical calculations.

We found two transition structures for the reaction channel leading to **4**-*cis* (labeled as **TS2**-*cis* and **TS2′**-*cis* in Figure 2) and two transition structures for the reaction channel leading to **4**-*trans* (labeled as **TS2**-*trans* and **TS2′**-*trans* in Figure 3). In the case of **TS2**-*cis* and **TS2′**-*cis*, their geometries differ one from the other essentially in the orientation of the O−O bond relative to the benzene cycle, **TS2**-*cis* with the O−O bond nearly eclipsing a C−C bond and **TS2′**-*cis* with the O−O bond pointing away from the ring. The geometry of **TS2**-*cis* is similar to that of the transition structure found at the UB3LYP/6-31(+)G(d) level reported in ref 26 (designated TS(B)). On the other hand, because the geometry of the transition structure found at the UB3LYP/6-31G(d) level for the O_2 addition to radical **1** affording the cis isomer of peroxyl radical **4** is not reported in ref 22, it is not possible to ascertain whether or not such a transition structure is identical to **TS2**-*cis*. However, the value of 5.0 kcal/mol calculated at UB3LYP/6-31G(d) level for the $\Delta H^{\ddagger}$(298 K) of this reaction pathway in ref 22 appears significantly higher than the value of 3.2 kcal/mol obtained at the same level of theory from data given in Table S4 (Supporting Information). It is likely that the transition structure found at the UB3LYP/6-31G(d) level for the O_2 addition to radical **1** yielding the cis isomer of peroxyl radical **4** in ref 22 corresponds to **TS2′**-*cis*.

The geometries of **TS2**-*trans* and **TS2′**-*trans* differ one from the other essentially in the orientation of the O−H bond relative to the benzene cycle, **TS2**-*trans* with the O−H bond pointing to the ring and **TS2′**-*trans* with the O−H bond pointing away from the ring. Earlier theoretical studies by Ghigo and Tonachini[23,26] on the **1** + O_2 → **4** reaction considered only the O_2 addition on the same side of the benzene ring as the OH group, affording the cis isomer of peroxyl radical **4**. Hence, the latter authors do not report any transition structure for the formation of the trans isomer of **4**. Furthermore, the geometry of the transition structure found for this reaction pathway by Lesclaux and co-workers is not reported in ref 22. Therefore, the geometries of either **TS2**-*trans* or **TS2′**-*trans* cannot be compared to that of any previously calculated transition structure.

The UB3LYP/6-31G(d) calculations predict that the total energy of **TS2**-*cis* is 2.5 kcal/mol lower than that of **TS2′**-*cis*, whereas the total energy of **TS2**-*trans* is 2.8 kcal/mol lower than that of **TS2′**-*trans* (see Table 2). At the UCCSD(T) level, these energy differences are found to be 4.2 and 2.4 kcal/mol, respectively. The $\langle S^2 \rangle$ values calculated for the UHF/6-311+G(2df,2p) wave function of **TS2**-*cis*, **TS2′**-*cis*, **TS2**-*trans*, and **TS2′**-*trans* are 2.04, 2.10, 2.04, and 2.06, respectively. As a consequence, the heights of the barriers computed with the UCCSD(T) and RCCSD(T) methods for the reaction channels affording either **4**-*cis* or **4**-*trans* should differ significantly. In fact, focusing on the lowest energy transition structure, the values of $\Delta U^{\ddagger}$ calculated with these methods are 6.6 and 1.5 kcal/mol (**TS2**-*cis*) and 6.4 and 1.5 kcal/mol (**TS2**-*trans*), respectively (see Table 2). The $\Delta U^{\ddagger}$ of 1.5 kcal/mol, calculated at the RCCSD(T) level for the reaction channels affording either **4**-*cis* or **4**-*trans*, leads to the rate coefficients at 298 K of 1.9×10^{-17} and 3.2×10^{-17} molecule^{-1} cm^3 s^{-1}, respectively (see Table 6). Thus, the RCCSD(T) calculations predict a global rate coefficient at 298 K of 5.1×10^{-17} molecule^{-1} cm^3 s^{-1} for the reaction yielding peroxyl radical **4**, which is a factor of about 15−25 lower than the experimental[21,22] values ranging between 7.7×10^{-16} and 13.1×10^{-16} molecule^{-1} cm^3 s^{-1}. On the other hand, the energy barriers of 6.6 and 6.4 kcal/mol, calculated at the UCCSD(T) level for the reaction channels affording **4**-*cis* and **4**-*trans*, respectively, lead to the rate coefficients at 298 K of 3.4×10^{-21} and 9.2×10^{-21} molecule^{-1} cm^3 s^{-1} (see Table 6). The UCCSD(T) calculations, therefore, predict a global rate coefficient at 298 K of 1.3×10^{-20} molecule^{-1} cm^3 s^{-1} for the reaction leading to peroxyl radical **4**, which is too low by a factor of 10^4−10^5 as compared to the experimental values. Thus, it appears that the RCCSD(T) method performs much better than the UCCSD(T) one in the calculation of the energy barriers for O_2 addition to position 2 of the benzene ring in **1** yielding peroxyl radical **4**. Again, this result is consistent with the fact that spin contamination is eliminated in the RCCSD(T) calculations.

At this point, it is worth noting that the rate coefficients at 298 K derived from the RCCSD(T) calculations indicate that the formation rate of **4**-*trans* is slightly faster (a factor of 1.7) than that of **4**-*cis* (see Table 6). This result is at variance with the theoretical calculations of Lesclaux and co-workers[22] predicting that the formation rate of the trans isomer is substantially faster (a factor of 50) than that of the cis one. This important discrepancy is traced back to the lower energy of **TS2**-*cis* as compared to that of the transition structure found by Lesclaux and co-workers for the reaction channel affording the cis isomer of peroxyl radical **4**.

Earlier energy calculations by Ghigo and Tonachini[23] concerning the O_2 addition to radical **1** yielding the cis isomer of peroxyl radical **4**, performed at the single-point UB3LYP/6-311+G(d,p) level using UB3LYP/6-31(+)G(d)-optimized geometries with energies corrected for spin contamination, are at variance with the results of our RCCSD(T) computations. Ghigo and Tonachini reported, in terms of ΔG(298 K), an energy barrier of 15.6 kcal/mol and an energy of reaction of 10.5 kcal/mol, which are significantly higher than the values of 13.9 and 1.4 kcal/mol we obtained at the RCCSD(T)/6-311+G(2df,2p) level. The origin of such a large discrepancy in the calculated energy of reaction is unclear. It has been observed in similar systems that the B3LYP functional may yield significant differences in calculated energies of reaction, as compared to the values obtained from CCSD(T) calculations.[22,62] In general, CCSD(T) calculations describe the reactions as being more exoergic than do B3LYP calculations.

3.3. Cyclization Reaction of Peroxyl Radical 4. On the basis of previous theoretical calculations of thermochemical and kinetic parameters for the cyclization of peroxyl radical **4** affording bicyclic radicals by formation of a peroxy bridge, the ring closure in **4** leading to radical **5** (see Scheme 3) appears to be the only possible cyclization pathway for peroxyl radical **4** under tropospheric conditions.[23] Therefore, here we have considered only this cyclization mode for both **4**-*cis* and **4**-*trans*. Table 3 gives the values of ΔU, ΔE(0 K), ΔH(298 K), and ΔG(298 K) calculated at different levels of theory for the relevant stationary points associated with these cyclization reactions. In agreement with the results of the theoretical study by Lesclaux and co-workers,[22] the UB3LYP, UCCSD(T), and RCCSD(T) calculations predict the cis stereoisomer of the byciclic radical **5** (labeled as **5**-*cis* in Figure 4) to be energetically more stable than the trans stereoisomer (labeled as **5**-*trans* in Figure 4). For instance, the values of ΔH(298 K) determined from the UCCSD(T) and RCCSD(T) calculations for **5**-*cis* are 4.6 and 4.7 kcal/mol, respectively, lower than those calculated for **5**-*trans*.

The transition structures calculated for the cyclization of **4**-*cis* leading to **5**-*cis* (labeled as **TS3**-*cis*) and the cyclization of **4**-*trans* affording **5**-*trans* (labeled as **TS3**-*trans*) are depicted in Figure 4. Interestingly, the $\Delta U^{\ddagger}$ values computed with the UCCSD(T) and RCCSD(T) methods for these reactions differ only in a few tenths of kcal/mol. This finding might be ascribed to a small degree of spin contamination of the UHF wave function of **TS3**-*cis* and **TS3**-*trans*. However, the $\langle S^2 \rangle$ value calculated for the UHF/6-311+G(2df,2p) wave function of **TS3**-*cis* and **TS3**-*trans* is 1.33.

Earlier UB3LYP/6-311+G(d,p) calculations using UB3LYP/6-31(+)G(d)-optimized geometries with energies corrected for spin contamination by Ghigo and Tonachini[23] on the ring closure of peroxyl radical **4** affording the bicyclic radical **5** considered only the cis isomer of **4**. The $\Delta H^{\ddagger}$(298 K) of 12.7 kcal/mol reported by Ghigo and Tonachini for this reaction pathway is in good agreement with the value of 12.4 kcal/mol we obtained from our RCCSD(T)/6-311+G(2df,2p) calculations. On the contrary, the ΔH_r(298 K) of -5.4 kcal/mol computed by Ghigo and Tonachini differs substantially from the value of -11.9 kcal/mol of our RCCSD(T)/6-311+G(2df,2p) calculations. We recall again that on similar systems it has been observed that, in general, the CCSD(T) calculations predict the reactions as being more exoergic than do the B3LYP calculations.[22,62]

In line with the results reported by Lesclaux and co-workers,[22] all barrier heights ($\Delta U^{\ddagger}$, $\Delta E^{\ddagger}$(0 K), $\Delta H^{\ddagger}$(298 K), and $\Delta G^{\ddagger}$(298 K)) calculated for the cyclization reaction of **4**-*cis* are significantly lower than those calculated for the cyclization of **4**-*trans* (see Table 3). As a consequence, the value of the rate coefficient at 298 K derived from the RCCSD(T) calculations (see Table 7) for the cyclization **4**-*cis* → **5**-*cis* (3.6×10^2 s^{-1}) is a factor of about 10^4 higher than the value determined for the cyclization **4**-*trans* → **5**-*trans* (4.1×10^{-2} s^{-1}). On the other hand, Table 7 shows that the rate coefficient calculated for the reversible decomposition **4**-*cis* → **1** + O_2 (5.1×10^3 s^{-1}) is about a factor of 10 higher than rate coefficient obtained for the cyclization **4**-*cis* → **5**-*cis*, whereas the rate coefficient for the reversible decomposition **4**-*trans* → **1** + O_2 (7.9×10^2 s^{-1}) is about a factor of 10^4 higher than the rate coefficient for the cyclization **4**-*trans* → **5**-*trans*. Therefore, under tropospheric conditions, it appears that the only possible reaction pathway for **4**-*trans* is the reversible decomposition back to the reactants, leading to the chemical equilibrium **1** + O_2 ↔ **4**-*trans*, whereas **4**-*cis* can undergo cyclization to the bicyclic radical **5**-*cis*. These results are pictorially illustrated in Figure 7 in terms of the ΔG(298 K) calculated at the RCCSD(T) level of theory for the relevant stationary points involved in the O_2 addition to position 2 of the benzene ring in radical **1** and the subsequent ring closure of the peroxyl radicals formed. Because the bicyclic radical **5** can lead readily to cleavage of the former aromatic ring yielding the principal benzene oxidation products (glyoxal and butenedial),[24,25] it turns out that the formation of **4**-*cis* implies irreversible loss of radical **1**. On the other hand, the experimentally observed chemical equilibrium **1** + O_2 ↔ **4** must essentially involve the trans isomer of peroxyl radical **4**. This feature confirms the assumption put forward by Lesclaux and co-workers[22] on the basis that the trans isomer is energetically more stable and is formed much more rapidly (a factor of about 50) than the cis one. However, as emphasized above, the rate coefficients at 298 K derived from the RCCSD(T) calculations indicate that the formation rate of **4**-*trans* is only slightly faster (a factor of 1.7) than that of **4**-*cis* (see Table 6). Therefore, the observed chemical equilibrium **1** + O_2 ↔ **4** must essentially involve the trans isomer of **4** because the cyclization **4**-*trans* → **5**-*trans* cannot compete with the decomposition of **4**-*trans* back to the reactants **1** + O_2.

3.4. O_2 Addition to Position 4 of the Benzene Ring in Hydroxycyclohexadienyl Radical. Table 4 gives the values of ΔU, ΔE(0 K), ΔH(298 K), and ΔG(298 K) calculated at different levels of theory for the relevant stationary points of the reaction pathway shown in Scheme 4. Both the UCCSD(T) and the RCCSD(T) calculations predict the total energy of the cis stereoisomer of peroxyl radical **6** (labeled as **6**-*cis* in Figure 5) to be 0.1 kcal/mol lower than that of the trans one (labeled as **6**-*trans* in Figure 5). Inclusion of ZPVE and thermal corrections to energy changes the relative energy ordering of these isomers. Thus, the ΔH(298 K) calculated at either the UCCSD(T) or the RCCSD(T) level of theory for **6**-*trans* is 1.9 kcal/mol lower than that of **6**-*cis*. The ΔH_r(298 K) values determined with the UCCSD(T) method for the addition reactions affording **6**-*cis* and **6**-*trans* (i.e., −10.4 and −12.3 kcal/mol, respectively) are 0.6 kcal/mol more negative than those calculated with the RCCSD(T) (i.e., −9.8 and −11.7 kcal/mol, respectively). Interestingly, these ΔH_r(298 K) values differ only in a few tenths of kcal/mol from those calculated for the addition reactions affording **4**-*trans* and **4**-*cis* (compare the ΔH(298 K) values given in Tables 2 and 4). As a consequence, the values of the equilibrium constants predicted for the chemical equilibriums **1** + O_2 ↔ **6**-*cis* and **1** + O_2 ↔ **6**-*trans* are close to those predicted for the equilibriums **1** + O_2 ↔ **4**-*cis* and **1** + O_2 ↔ **4**-*trans*, respectively (see Table 8).

At variance with the addition reactions **1** + O_2 affording **4**-*cis* and **4**-*trans*, we found only one transition structure for the reaction channel leading to **6**-*cis* (labeled as **TS4**-*cis* in Figure 5) and only one transition structure for the reaction channel leading to **6**-*trans* (labeled as **TS4**-*trans* in Figure 5). The UB3LYP/6-31G(d) calculations predict that the total energy of **TS4**-*cis* is 0.2 kcal/mol higher than that of **TS4**-*trans* (see Table 4). At the UCCSD(T) level of theory, the total energy of **TS4**-*cis* is calculated to be 0.1 kcal/mol lower than that of **TS4**-*trans*. The $\langle S^2 \rangle$ values determined for the UHF/6-311+G(2df,2p) wave functions of **TS4**-*cis* and **TS4**-*trans* are 1.98 and 1.99, respectively. As a consequence, the heights of the barriers computed with the UCCSD(T) and RCCSD(T) methods for the reaction channels leading to **6**-*cis* and **6**-*trans* differ significantly. For instances, the values of $\Delta U^{\ddagger}$ calculated with the UCCSD(T) and RCCSD(T) methods for these reaction channels are 8.1 and 4.6 kcal/mol (**TS4**-*cis*) and 8.2 and 4.8 kcal/mol (**TS4**-*trans*), respectively (see Table 4).

Focusing on the energy barriers calculated with the RCCSD(T) method, a comparison between the O_2 addition to positions 2 and 4 of the benzene ring in radical **1** affording the cis and trans isomers of radicals **4** and **6** reveals that the $\Delta U^{\ddagger}$ for the addition to position 4 is about 3 kcal/mol higher than that for addition to position 2 (see Tables 2 and 4). The energy barriers determined from the RCCSD(T) calculations for the reaction channels affording **6**-*cis* and **6**-*trans* lead to the rate coefficients at 298 K of 2.1×10^{-18} and 1.3×10^{-18} molecule^{-1} cm^3 s^{-1}, respectively, which are a factor of about 10 lower than those calculated for the reaction channels affording **4**-*cis* and **4**-*trans* (see Table 6). Consequently, although the ΔH_r(298 K) values for the O_2 addition to positions 2 and 4 of the benzene ring in radical **1** are predicted to be similar, the addition to position 2 is clearly preferred over the addition to position 4.

3.5. Cyclization Reaction of Peroxyl Radical 6. From the strain energy point of view, the ring closure to the bicyclic radical **7** (see Scheme 5) appears to be the more viable cyclization mode of peroxyl radical **6** under tropospheric conditions. Therefore, here we have considered only this cyclization mode for both **6**-*cis* and **6**-*trans*. Table 5 gives the values of ΔU, ΔE(0 K), ΔH(298 K), and ΔG(298 K) calculated at different levels of theory for the relevant stationary points associated with these cyclization reactions. Both the UCCSD(T) and the RCCSD-(T) calculations predict the cis stereoisomer of the byciclic radical **7** (labeled as **7**-*cis* in Figure 6) to be energetically more stable than the trans stereoisomer (labeled as **7**-*trans* in Figure 6). Thus, the ΔH(298 K) values determined from the UCCSD(T) and RCCSD(T) calculations for **7**-*cis* are 5.0 and 4.9 kcal/mol lower, respectively, than those calculated for **7**-*trans*.

In clear contrast with the cyclization reactions **4**-*cis* → **5**-*cis* and **4**-*trans* → **5**-*trans*, which were found to be exothermic, the cyclizations **6**-*cis* → **7**-*cis* and **6**-*trans* → **7**-*trans* are calculated to be endothermic. For instance, the ΔH_r(298 K) values determined from the RCCSD(T) calculations for the reactions **4**-*cis* → **5**-*cis* and **4**-*trans* → **5**-*trans* are −11.9 and −7.2 kcal/mol, respectively (see Table 3), whereas those determined for the reactions **6**-*cis* → **7**-*cis* and **6**-*trans* → **7**-*trans* are 7.1 and 12.0 kcal/mol, respectively (see Table 5).

The transition structures found for the cyclization reactions **6**-*cis* → **7**-*cis* (labeled as **TS5**-*cis*) and **6**-*trans* → **7**-*trans* (labeled as **TS5**-*trans*) are shown in Figure 6. Although the $\langle S^2 \rangle$ values calculated for the UHF/6-311+G(2df,2p) wave function for **TS5**-*cis* (1.14) and **TS5**-*trans* (1.15) indicate a significant degree of spin contamination, the $\Delta U^{\ddagger}$ values computed with the UCCSD(T) and RCCSD(T) methods for these reactions are similar (see Table 5). As found for the cyclization reactions of **4**-*cis* and **4**-*trans*, all barrier heights ($\Delta U^{\ddagger}$, $\Delta E^{\ddagger}$(0 K), $\Delta H^{\ddagger}$(298 K), and $\Delta G^{\ddagger}$(298 K)) calculated for the cyclization of **6**-*cis* are significantly lower than those calculated for the cyclization of **6**-*trans* (see Table 5). However, all barrier heights computed for the cyclization of either **6**-*cis* or **6**-*trans* are about twice those computed for the cyclization of either **4**-*cis* or **4**-*trans* (see Tables 3 and 5). Furthermore, the values of the rate coefficient at 298 K derived from the RCCSD(T) calculations (see Table 7) for the cyclizations **6**-*cis* → **7**-*cis* (7.7×10^{-11} s^{-1}) and **6**-*trans* → **7**-*trans* (4.9×10^{-14} s^{-1}) are extremely small, as compared to those for the cyclizations **4**-*cis* → **5**-*cis* (3.6×10^{2} s^{-1}) and **4**-*trans* → **5**-*trans* (4.1×10^{-2} s^{-1}). On the other hand, Table 7 shows that the rate coefficient calculated for the reversible decomposition **6**-*cis* → **1** + O_2 (2.8×10^{2} s^{-1}) is about a factor of 10^{13} higher than the rate coefficient obtained for the cyclization **6**-*cis* → **7**-*cis* and the rate coefficient for the reversible decomposition **6**-*trans* → **1** + O_2 (6.8×10^{1} s^{-1}) is about a factor of 10^{15} higher than the rate coefficient for the cyclization **6**-*trans* → **7**-*trans*. Therefore, under tropospheric conditions, it appears that the only possible reaction pathway for either **6**-*cis* or **6**-*trans* is the reversible decomposition back to the reactants, leading to the chemical equilibrium **1** + O_2 ↔ **6**. This feature is pictorially illustrated in Figure 8 in terms of the ΔG(298 K) calculated at the RCCSD(T) level of theory for the stationary points involved in the O_2 addition to position 4 of the benzene ring in radical **1** and the subsequent ring closure of the peroxyl radicals formed. As a consequence, it appears that the O_2 addition to position 4 of the benzene ring in radical **1** cannot contribute to the formation of benzene oxidation products through cleavage of the former aromatic ring in bicyclic radicals **7**-*cis* and **7**-*trans*.

3.6. Global Irreversible Loss of Hydroxycyclohexadienyl and Peroxyl Radicals. One of the main objectives of the experimental work carried out by Lesclaux and co-workers[22] on the reaction of radical **1** with O_2 was to provide kinetic data accounting for the global irreversible loss of radical species (essentially radical **1** and the resulting peroxyl radicals), yielding phenol and other oxidation products. Specifically, Lesclaux and co-workers measured experimentally a total rate coefficient for the global radical loss reactions of $(2.52 \pm 0.40) \times 10^{-16}$ cm^3 molecule^{-1} s^{-1} at 295 K. This rate coefficient was employed for evaluating product yields from calculated rate coefficients of possible reaction channels. In particular, from the rate coefficient at 298 K of 1.4×10^{-16} molecule^{-1} cm^3 s^{-1} calculated for the phenol channel, a yield of about 55% was obtained for phenol, in reasonable agreement with experimental values (25−61%).[1,30−32]

Besides the reaction channel yielding phenol, the theoretical results described above for the possible reaction channels arising from the reaction of radical **1** with O_2 indicate that the reaction channel **1** + O_2 → **4**-*cis* is the only reaction leading to irreversible loss of radical **1**. Therefore, excluding radical−radical reactions, the total rate coefficient for the global irreversible loss of radicals species can be approximated as the sum of the rate coefficients at 298 K calculated for the reactions **1** + O_2 → **3** + $HOO^•$ and **1** + O_2 → **4**-*cis*. This approximation leads to a total rate coefficient at 298 K of 2.3×10^{-17} molecule^{-1} cm^3 s^{-1} (see Table 6), which is a factor of about 10 lower than the experimental value of Lesclaux and co-workers. However, from the rate coefficient at 298 K of 4.2×10^{-18} molecule^{-1} cm^3 s^{-1} calculated for the phenol channel, a yield of about 18% was obtained for phenol, in reasonable agreement with experimental values.[1,30−32] Therefore, although the energy barriers obtained from RCCSD(T) calculations with the 6-311+G (2df,2p) basis set for the competing reaction channels arising from the reaction **1** + O_2 lead to rate coefficients at 298 K that are a factor of about 10 too low, the relative rate coefficients are reasonably reliable.

3.7. Comparison to Theoretical Calculations on $HO^•$-Initiated Oxidation of *p*-Xylene and *m*-Xylene. Recently, Fan and Zhang have studied the $HO^•$-initiated oxidation reactions of *p*-xylene[63] and *m*-xylene.[64] By using optimized geometries, vibrational frequencies, and ZPVE-corrected energies, obtained at the UB3LYP/6-31G(d,p) level, Fan and Zhang have investigated the competing pathways arising from the reaction of the *p*-xylene−$HO^•$ and *m*-xylene−$HO^•$ adducts with O_2 to assess the energetically favorable pathways to propagate the oxidations. As compared to benzene oxidation, the mechanistic complexity of the *p*-xylene and *m*-xylene oxidations is much higher due to the existence of multiple isomeric pathways at each reaction stage.

The theoretical calculations of Fan and Zhang predict the $HO^•$ addition to occur preferentially at the ortho position of *p*-xylene and the two possible ortho positions of *m*-xylene. Regarding the O_2 addition to the *p*-xylene−$HO^•$ and *m*-xylene−$HO^•$ adducts, the theoretical study of Fang and Zhang focuses exclusively on the addition on the same side of the benzene ring as the hydroxyl group, because they found that this addition mode leads to the formation of the energetically favorable isomers of the peroxyl radicals. In clear contrast, our UCCSD(T) and RCCSD(T) calculations predict that the peroxyl radical **4**-*trans* resulting from the O_2 addition to the benzene−$HO^•$ adduct **1** is less energetic and is formed somewhat faster than the isomer **4**-*cis*.

The ZPVE-corrected reaction energies (designated by ΔE_r(0 K)) for the formation of $HO^•$−*p*-xylene−O_2 and $HO^•$−*m*-xylene−O_2 peroxyl radicals from the O_2 addition to the corresponding *p*-xylene−$HO^•$ and *m*-xylene−$HO^•$ adducts range from −4.5 to −7.1 kcal/mol. These values are significantly less negative than the ΔE_r(0 K) obtained from the UCCSD(T) and RCCSD(T) calculations (see Tables 2 and 4) for the reaction pathways **1** + O_2 → **4**-*cis* (−10.1 and −9.4 kcal/mol, respectively) and **1** + O_2 → **6**-*cis* (−9.6 and −9.0 kcal/mol, respectively). The ZPVE-corrected energy barriers (designated by $\Delta E^‡$(0 K)) for the O_2 addition to the ortho *p*-xylene−$HO^•$ adduct range from −0.51 to 4.18 kcal/mol, while for the O_2 addition to the two ortho *p*-xylene−$HO^•$ adducts range from −1.2 to 3.56 kcal/mol. These barriers are lower than our $\Delta E^‡$(0 K) values of 3.3 and 6.0 kcal/mol obtained with the RCCSD(T) method for the reaction pathways **1** + O_2 → **4**-*cis* and **1** + O_2 → **6**-*cis*, respectively.

Finally, it is worth noting that the ΔE_r(0 K) values reported by Fan and Zhang for the cyclization of the *p*-xylene and *m*-xylene peroxyl radicals arising from initial $HO^•$ and subsequent O_2 addition to the ring to form bridged bicyclic radicals possessing a delocalized allyl system range between −5.37 and −8.89 kcal/mol. These values are less negative than the ΔE_r(0 K) obtained from the UCCSD(T) and RCCSD(T) calculations (see Table 3) for the isomerization of peroxyl radical **4**-*cis* to the bicyclic radical **5**-*cis* (−10.5 and −11.4 kcal/mol, respectively). Furthermore, the $\Delta E^‡$(0 K) values reported by Fan and Zhang for the cyclization of $HO^•$−*p*-xylene−O_2 and $HO^•$−*m*-xylene−O_2 peroxyl radicals affording bridged bicyclic radicals containing a delocalized allyl radical (ranging from 9.07 to 11.14 kcal/mol) are significantly lower than the $\Delta E^‡$(0 K) value of 13.1 kcal/mol predicted by the RCCSD(T) calculations for the isomerization of peroxyl radical **4**-*cis* to the bicyclic radical **5**-*cis*.

4. Summary and Conclusions

Density functional theory (UB3LYP) and quantum-mechanical (UCCSD(T) and RCCSD(T)) electronic structure calculations were carried out to investigate the primary steps of the oxidative degradation of benzene under tropospheric conditions, initiated by the addition of $HO^•$ to the aromatic ring. The energetic, structural, and vibrational results furnished by these calculations were subsequently used to perform conventional transition-state computations to predict the rate coefficients and evaluate the product yields of the competing abstraction and addition reactions arising from the reaction of the benzene−$HO^•$ adduct **1** with O_2. From the analysis of the results, the following main points emerge.

(1) The barrier heights ($\Delta U^‡$, $\Delta E^‡$, $\Delta H^‡$, and $\Delta G^‡$) determined from RCCSD(T) calculations with the 6-311+G(2df,2p) basis set are found to be more reliable than those obtained from UCCSD(T) calculations with the same basis set. This theoretical finding is ascribed to the high degree of spin contamination shown by the UHF wave function underlying the UCCSD(T) calculations of the transition structures and is consistent with the fact that such spin contamination is eliminated in the RCCSD(T) calculations.

(2) It is confirmed that the trans stereoisomer of the peroxyl radical **4** produced by the O_2 addition to position 2 of benzene ring in the benzene−$HO^•$ adduct **1** is energetically more stable than the cis one. However, at variance with an earlier theoretical study, the rate coefficients at 298 K for the formation of both stereoisomers are predicted to be similar.

(3) All of the barrier heights ($\Delta U^‡$, $\Delta E^‡$, $\Delta H^‡$, and $\Delta G^‡$) calculated for the cyclization of the cis isomer of peroxyl radical **4** to the cis isomer of a bicyclic allyl radical **5** bearing a peroxy bridge are significantly lower than those calculated for the cyclization of the trans isomer of **4**. Because radical **5** can lead readily to cleavage of the former aromatic ring yielding the principal benzene oxidation products, it is concluded that the formation of the cis isomer of **4** implies irreversible loss of radical **1** and that the observed chemical equilibrium **1** + $O_2 \leftrightarrow$ **4** must essentially involve the trans isomer of **4**.

(4) The O_2 addition to position 4 of benzene ring in the benzene−$HO^•$ adduct **1** affords the cis and trans stereoisomers of a peroxyl radical **6**. The cis isomer of **6** is predicted to be energetically more stable than the trans one. Although the reaction enthalpies calculated for the O_2 addition to positions 2 and 4 of the benzene ring in radical **1** are calculated to be similar, the addition to position 2 is clearly preferred over the addition to position 4 because it involves a lower barrier.

(5) The heights of the barriers computed for the cyclization of either the cis or the trans isomer of peroxyl radical **6** to a bicyclic radical **7** bearing a peroxy bridge are about twice the heights of the barriers computed for the cyclization of either the cis or the trans isomer of peroxyl radical **4** to bicyclic radical **5**. Under tropospheric conditions, the only possible reaction pathway for radical **6** is the reversible decomposition back to the reactants, leading to the chemical equilibrium **1** + $O_2 \leftrightarrow$ **6**. As a consequence, it is unlikely that the O_2 addition to position 4 of the benzene ring in radical **1** can contribute to the formation of benzene oxidation products.

Acknowledgment. This research was supported by the Spanish MEC (Grants CTQ2005-07790-C02-01 and CTQ2005-01117). Additional support came from the Catalonian AGAUR (Grants 2005SGR00111 and 2005PEIR0051/69). The larger calculations described in this work were performed at the Centre de Supercomputació de Catalunya (CESCA). The reviewers provided helpful comments for improving this Article.

Supporting Information Available: The $\langle S^2 \rangle$ values of the UHF/6-311+G(2df,2p) wave functions, open-shell T_1 diagnostic values of the RCCSD calculations, total energies, zero-point vibrational energies, and thermal corrections to enthalpy and Gibbs energy, as well as the Cartesian coordinates of all structures reported in this Article. This material is available free of charge via the Internet at http://pubs.acs.org.

References

(1) Calvert, J. G.; Atkinson, R.; Becker, K. H.; Kamens, R. M.; Seinfeld, J. H.; Wallington, T. J.; Yarwood, G. *The Mechanism of Atmospheric Oxidation of Aromatic Hydrocarbons*; Oxford University Press: New York, 2002.

(2) Piccot, S. D.; Watson, J. J.; Jones, J. W. *J. Geophys. Res.* **1992**, *97*, 9897.

(3) Legett, S. *Atmos. Environ.* **1996**, *30*, 215.

(4) Derwent, R. G.; Jenkin, M. E.; Saunders, S. M. *Atmos. Environ.* **1996**, *30*, 181.

(5) Seinfeld, J. H.; Pandis, S. N. *Atmospheric Chemistry and Physics: From Air Pollution to Climate Change*; John Wiley & Sons: New York, 1997.

(6) Lay, T. H.; Bozzelli, J. W.; Seinfeld, J. H. *J. Phys. Chem.* **1996**, *100*, 6543.

(7) Atkinson, R.; Aschmann, S. M. *Int. J. Chem. Kinet.* **1994**, *26*, 929.

(8) Atkinson, R.; Aschmann, S. M.; Arey, J.; Carter, W. P. L. *Int. J. Chem. Kinet.* **1989**, *21*, 801.

(9) Semadeni, M.; Stocker, D. W.; Kerr, J. A. *Int. J. Chem. Kinet.* **1995**, *27*, 287.

(10) Wallington, T. J.; Neuman, D. J.; Kurylo, M. J. *Int. J. Chem. Kinet.* **1987**, *19*, 725.

(11) Witte, F.; Urbanik, E.; Zetzsch, C. *J. Phys. Chem.* **1986**, *90*, 3251.

(12) Knispel, R.; Koch, R.; Seise, M.; Zetzsch, C. *Ber. Bunsen-Ges. Phys. Chem.* **1990**, *94*, 1375.

(13) Lin, S.-C.; Kuo, T.-C.; Lee, Y.-P. *J. Chem. Phys.* **1994**, *101*, 2098.

(14) Bjergbakke, E.; Sillesen, A.; Pagsberg, P. J. *J. Phys. Chem.* **1996**, *100*, 5729.

(15) Zellner, R.; Fritz, B.; Priedel, M. *Chem. Phys. Lett.* **1985**, *121*, 412.

(16) Zetzsh, C.; Koch, R.; Bohn, B.; Knispel, R.; Siese, M.; Witte, F. In *Transp. Chem. Transform. Pollut. Troposphere*; Le

Bras, G., Ed.; Springer: Berlin, Germany, 1997; Vol. 3, pp 347−356.

(17) Approximate atmospheric concentrations of the reactive species can be found, for example, in: (a) Güsten, H. Degradation of Atmospheric Pollutants by Tropospheric Free Radical Reactions. In *Free Radicals in Biology and Environment*; Minisci, F., Ed.; Kluwer Academic Publishers: The Netherlands, 1997; Chapter 28, pp 387−408. (b) Atkinson, R. Reactions of Oxygen Species in the Atmosphere. In *Active Oxygen in Chemistry*; Valentine, J. S., Foote, C. S., Greenberg, A., Liebman, J. F., Eds.; Blackie Academic and Professional: New York, 1995; Chapter 7. (c) Wayne, R. P. *Chemistry of Atmospheres*; Clarendon Press: Oxford, UK, 1996; pp 252−263.

(18) Bohn, B.; Zetzsch, C. *Phys. Chem. Chem. Phys.* **1999**, *1*, 5097.

(19) Bohn, B. *J. Phys. Chem. A* **2001**, *105*, 6092.

(20) Johnson, S.; Raoult, S.; Rayez, M. T.; Rayez, J. C.; Lesclaux, R. *Phys. Chem. Chem. Phys.* **2002**, *4*, 4678.

(21) Grebenkin, S. Y.; Krasnoperov, L. N. *J. Phys. Chem. A* **2004**, *108*, 1953.

(22) Raoult, S.; Rayez, M. T.; Rayez, J. C.; Lesclaux, R. *Phys. Chem. Chem. Phys.* **2004**, *6*, 2245.

(23) Ghigo, G.; Tonachini, G. *J. Am. Chem. Soc.* **1999**, *121*, 8366.

(24) Tuazon, E. C.; MacLeod, H.; Atkinson, R.; Carter, W. P. L. *Environ. Sci. Technol.* **1986**, *20*, 383.

(25) Volkamer, R.; Platt, U.; Wirtz, K. *J. Phys. Chem. A* **2001**, *105*, 7865.

(26) Ghigo, G.; Tonachini, G. *J. Am. Chem. Soc.* **1998**, *120*, 6753.

(27) Motta, F.; Ghigo, G.; Tonachini, G. *J. Phys. Chem. A* **2002**, *106*, 4411.

(28) Marcus, R. A. *J. Phys. Chem.* **1968**, *72*, 891.

(29) Rayez, M. T.; Rayez, J. C.; Sawerysyn, J. P. *J. Phys. Chem.* **1994**, *98*, 11342.

(30) Berndt, T.; Böge, O. *Phys. Chem. Chem. Phys.* **2001**, *3*, 4946.

(31) Volkamer, R.; Klotz, B.; Barnes, I.; Imamura, T.; Wirtz, K.; Washida, N.; Becker, K. H.; Platt, U. *Phys. Chem. Chem. Phys.* **2002**, *4*, 1598.

(32) Berndt, T.; Böge, O. *Phys. Chem. Chem. Phys.* **2006**, *8*, 1205.

(33) (a) Atkinson, R.; Carter, W. P. L.; Darnell, K. R.; Winer, A. M.; Pitts, J. N. *Int. J. Chem. Kinet.* **1980**, *12*, 779. (b) Atkinson, R.; Lloyd, A. C. *J. Phys. Chem. Ref. Data* **1984**, *13*, 315.

(34) (a) Schlegel, H. B. *J. Comput. Chem.* **1982**, *3*, 214. (b) Bofill, J. M. *J. Comput. Chem.* **1994**, *15*, 1.

(35) Becke, A. D. *J. Chem. Phys.* **1993**, *98*, 5648.

(36) Lee, C.; Yang, W.; Parr, R. G. *Phys. Rev. B* **1988**, *37*, 785.

(37) Stevens, P. J.; Devlin, F. J.; Chablowski, C. F.; Frisch, M. J. *J. Phys. Chem.* **1994**, *98*, 11623.

(38) Hariharan, C.; Pople, J. A. *Theor. Chim. Acta* **1973**, *28*, 213.

(39) (a) Fukui, K. *Acc. Chem. Res.* **1981**, *14*, 363. (b) Ishida, K.; Morokuma, K.; Kormornicki, A. *J. Chem. Phys.* **1977**, *66*, 2153.

(40) (a) Gonzalez, C.; Schlegel, H. B. *J. Chem. Phys.* **1989**, *90*, 2154. (b) Gonzalez, C.; Schlegel, H. B. *J. Phys. Chem.* **1990**, *94*, 5523.

(41) Hehre, W. J.; Radom, L.; Schleyer, P. v. R.; Pople, J. A. *Ab Initio Molecular Orbital Theory*; John Wiley: New York, 1986; pp 86−87.

(42) For a review, see: Roos, B. O. *Adv. Chem. Phys.* **1987**, *69*, 399.

(43) See, for example: Zhao, J.; Zhang, R. *Adv. Quantum Chem.* **2008**, *55*, 177–213.

(44) For a review, see: Bartlett, R. J. *J. Phys. Chem.* **1989**, *93*, 1967.

(45) Raghavachari, K.; Trucks, G. W.; Pople, J. A.; Head-Gordon, M. *Chem. Phys. Lett.* **1989**, *157*, 479.

(46) Frisch, M. J.; Pople, J. A.; Binkley, J. S. *J. Chem. Phys.* **1984**, *80*, 3265.

(47) Knowles, P. J.; Hampel, C.; Werner, H.-J. *J. Chem. Phys.* **1993**, *99*, 5219.

(48) (a) Purvis, G. D.; Bartlett, R. J. *J. Chem. Phys.* **1982**, *76*, 1910. (b) Hampel, C.; Peterson, K. A.; Werner, H.-J. *Chem. Phys. Lett.* **1992**, *190*, 1. (c) Deegan, M. J. O.; Knowles, P. J. *Chem. Phys. Lett.* **1994**, *227*, 321.

(49) Jayatilaka, D.; Lee, T. J. *J. Chem. Phys.* **1993**, *98*, 9734.

(50) Rienstra-Kiracofe, J. C.; Allen, W. D.; Schaefer, H. F., III. *J. Phys. Chem. A* **2000**, *104*, 9823.

(51) (a) Anderson, K.; Malmqvist, P.-A.; Roos, B. O.; Sadlej, A. J.; Wolinski, K. *J. Phys. Chem.* **1990**, *94*, 5483. (b) Anderson, K.; Malmqvist, P.-A.; Roos, B. O. *J. Chem. Phys.* **1992**, *96*, 1218.

(52) McQuarrie, D. *Statistical Mechanics*; Harper and Row: New York, 1986.

(53) Frisch, M. J.; Trucks, G. W.; Schlegel, H. B.; Scuseria, G. E.; Robb, M. A.; Cheeseman, J. R.; Montgomery, J. A., Jr.; Vreven, T.; Kudin, K. N.; Burant, J. C.; Millam, J. M.; Iyengar, S. S.; Tomasi, J.; Barone, V.; Mennucci, B.; Cossi, M.; Scalmani, G.; Rega, N.; Petersson, G. A.; Nakatsuji, H.; Hada, M.; Ehara, M.; Toyota, K.; Fukuda, R.; Hasegawa, J.; Ishida, M.; Nakajima, T.; Honda, Y.; Kitao, O.; Nakai, H.; Klene, M.; Li, X.; Knox, J. E.; Hratchian, H. P.; Cross, J. B.; Adamo, C.; Jaramillo, J.; Gomperts, R.; Stratmann, R. E.; Yazyev, O.; Austin, A. J.; Cammi, R.; Pomelli, C.; Ochterski, J. W.; Ayala, P. Y.; Morokuma, K.; Voth, G. A.; Salvador, P.; Dannenberg, J. J.; Zakrzewski, V. G.; Dapprich, S.; Daniels, A. D.; Strain, M. C.; Farkas, O.; Malick, D. K.; Rabuck, A. D.; Raghavachari, K.; Foresman, J. B.; Ortiz, J. V.; Cui, Q.; Baboul, A. G.; Clifford, S.; Cioslowski, J.; Stefanov, B. B.; Liu, G.; Liashenko, A.; Piskorz, P.; Komaromi, I.; Martin, R. L.; Fox, D. J.; Keith, T.; Al-Laham, M. A.; Peng, C. Y.; Nanayakkara, A.; Challacombe, M.; Gill, P. M. W.; Johnson, B.; Chen, W.; Wong, M. W.; Gonzalez, C.; Pople, J. A. *Gaussian 03*, revision C.02; Gaussian, Inc.: Wallingford, CT, 2004.

(54) Werner, H.-J.; Knowles, P. J.; Almlöf, J.; Amos, R. D.; Berning, A.; Cooper, D. L.; Deegan, M. J. O.; Dobbyn. A. J.; Eckert, S. T.; Hampel, C.; Leininger, C.; Lindh, R.; Lloyd, A. W.; Meyer, W.; Mura, M. E.; Nicklass, A.; Palmieri, P.; Peterson, K. A.; Pitzer, R.; Pulay, P.; Rauhaut, G.; Schütz, M.; Stoll, H.; Stone, A. J.; Thorsteinsson, T. *MOLPRO, version 98.1*; University of Stuttgart: Germany, 1998.

(55) Schmidt, M. W.; Baldrige, K. K.; Boatz, J. A.; Elbert, S. T.; Gordon, M. S.; Jensen, J.; Koseki, S.; Matsunaga, N.; Nguyen, K. A.; Su, S.; Windus, T. L.; Dupuis, M.; Montgomery, J. A. *J. Comput. Chem.* **1993**, *14*, 1347.

(56) Karlström, G.; Lindh, R.; Malmqvist, P.-Å.; Roos, B. O.; Ryde, U.; Veryazov, V.; Widmark, P.-O.; Cossi, M.; Schimmelpfen-

nig, B.; Neogrády, P.; Seijo, L. *Comput. Mater. Sci.* **2003**, *28*, 222.

(57) Eyring, H. *J. Chem. Phys.* **1935**, *107*, 107.

(58) Truong, T. N.; Truhlar, D. G. *J. Chem. Phys.* **1990**, *93*, 1761.

(59) Eckart, C. *Phys. Rev.* **1930**, *35*, 1303.

(60) Benson, S. W. *Thermochemical Kinetics*; Wiley & Sons: New York, 1976; p 8.

(61) (a) Bader, R. F. W. *Atoms in Molecules: A Quantum Theory*; Clarendon: Oxford, UK, 1990. (b) Matta, C. F.; Boyd, R. J. An Introduction to the Quantum Theory of Atoms in Molecules. In *The Quantum Theory of Atoms in Molecules*, 1st ed.; Matta, C. F., Boyd, R. J., Eds.; Wiley−VCH: Weinheim, Germany, 2007; pp 1−34.

(62) Suh, I.; Zhang, R.; Molina, L. T.; Molina, M. J. *J. Am. Chem. Soc.* **2003**, *125*, 12655.

(63) Fan, J.; Zhang, R. *J. Phys. Chem. A* **2006**, *110*, 7728.

(64) Fan, J.; Zhang, R. *J. Phys. Chem. A* **2008**, *112*, 4314.

CT900082G